Phase transitions in open quantum systems

C. Jung^{1,2}, M. Müller^{1,3} and I. Rotter^{1,4}

Centro Internacional de Ciencias, Cuernavaca, Mexico
 Instituto de Matematicas, Unidad Cuernavaca, UNAM
 Apdo. postal 273-3, 62151 Cuernavaca, Mexico
 Max-Planck-Institut für Physik komplexer Systeme
 Nöthnitzer Str. 38, D-01187 Dresden, Germany
 Technische Universität Dresden, Institut für Theoretische Physik,
 D-01062 Dresden, Germany, and
 Max-Planck-Institut für Physik komplexer Systeme
 Nöthnitzer Str. 38, D-01187 Dresden, Germany

05.70.Fh, 03.80.+r, 64.60.-i, 03.65.-w

Abstract

We consider the behaviour of open quantum systems in dependence on the coupling to one decay channel by introducing the coupling parameter α being proportional to the average degree of overlapping. Under critical conditions, a reorganization of the spectrum takes place which creates a bifurcation of the time scales with respect to the lifetimes of the resonance states. We derive analytically the conditions under which the reorganization process can be understood as a second-order phase transition and illustrate our results by numerical investigations. The conditions are fulfilled e.g. for a picket fence with equal coupling of the states to the continuum. Energy dependencies within the system are included. We consider also the generic case of an unfolded Gaussian Orthogonal Ensemble. In all these cases, the reorganization of the spectrum occurs at the critical value $\alpha_{\rm crit}$ of the control parameter globally over the whole energy range of the spectrum. All states act cooperatively.

1 Introduction

Recently, the properties of open quantum systems have been studied with a renewed interest in the framework of different approaches. Mostly discussed is the restructuring of the systems taking place at high level density under critical conditions and the resulting formation of different time scales in terms of lifetimes of resonance states. The reorganization occurs if the degree $\bar{\Gamma}/\bar{D}$ of overlapping reaches a critical value ($\bar{\Gamma}$ is the average width obtained by averaging over all M resonance states in a certain energy region and \bar{D} is the mean level distance). It is investigated for resonance phenomena in nuclei [1, 2, 3, 4, 5, 6], atoms [7, 8] and molecules [9]. In the meantime it has been considered also in other systems such as e.g. quantum dots [10] and microwave billards [11]. The number M of resonance states is usually much larger than the number K of open decay channels.

A powerful method in describing the properties of an open quantum system is the projection operator technique. It allows us to investigate, in a direct manner, the corrections to the many-particle states in a subspace of the full Hilbert space which arise from the coupling to the orthogonal subspace. Originally the idea of using the projection operator technique arose in nuclear physics. The influence of discrete states as well as closed decay channels (Q subspace) onto the wavefunctions of the open decay channels (P subspace) is considered in the Feshbach unified theory of nuclear reactions [12]. This phenomenological model describes well the properties of nuclei at an excitation energy of about 10 MeV by employing statistical assumptions on the states of the Q subspace. In contrast to this, the ground and low-lying states of nuclei are described well by the wavefunctions of the discrete states (Q subspace), considering the influence of the decay channels (P subspace) in an approximated manner.

The properties of an *open* quantum system are described well by using the latter division of the whole function space: the Q subspace contains the discrete states of the system while the P subspace consists of open as well as closed decay channels [1]. In studying the restructuring, we are interested in the properties of the states of the Q subspace modified by their coupling to the P subspace playing the role of an environment. This method can be used for a wide class of open quantum systems [13].

The question whether this restructuring may be considered as a phase transition of second order is put in [3] but not considered in detail up to now. A possible analogy to the formation of laser light is investigated numerically in [4]. As in the case of the laser, a control parameter α can be defined which is proportional to $\bar{\Gamma}/\bar{D}$. The information entropy changes rapidly in a relatively small region of the control parameter in both the laser [14] and the open quantum system [4].

In other investigations [5] it was realized that the avoided crossing of two neighbouring resonance states which are coupled to one common channel is the basic process of the restructuring observed globally in the system. As soon as two resonances start to overlap each other, their interaction via the continuum can no longer be neglected. As a function of the coupling to a certain decay channel the two resonances approach each other in energy up to a certain minimum distance in the complex energy plane at $\alpha = \alpha_{\rm crit}$. The avoided crossing is reflected in the wavefunctions of the two resonance states. The biorthogonality reaches its maximum if $\alpha \to \alpha_{\rm crit}$, and vanishes if $\alpha \to 0$ and $\alpha \to \infty$ [5]. As a function of further increasing $\alpha > \alpha_{\rm crit}$, the width of one of the two resonance states decreases (resonance trapping) while the width of

the other one increases further.

The local resonance trapping can explain, indeed, the global restructuring of the quantum system under critical conditions. It determines also, as will be shown in this paper, whether the restructuring of the system takes place collectively with the simultaneous participation of all basis states or successively by individual trapping of resonance states.

In the following, we will investigate this question in detail. In sect. 2, we write down the basic equations used in the paper. The model is formulated and the characteristic polynomial is given. The Hamiltonian is non-hermitian and its eigenfunctions are, generally, bi-orthogonal. In section 3, the properties of a system with picket-fence distributed levels coupled with the same strength to one decay channel is investigated in detail. The study is performed analytically for the limiting case of an infinite number of states as well as for a finite number. The results are illustrated by numerical calculations. Finally, the results obtained are discussed and identified with characteristic features of a second-order phase transition. The process of formation of a collective state aligned with the decay channel is discussed in detail. Its wavefunction is coherently mixed in the wavefunctions of all basis states including those states which are *not* overlapped by it.

The results obtained in section 3 are underpinned in section 4 by considering some other level and coupling-strength distributions being more realistic than those in section 3. The study is performed both analytically and numerically. General conditions for the appearance of a second-order phase transition are formulated analytically and illustrated by the results of numerical calculations. As a special case, the sharpness of a phase transition is shown to be distorted by an imaginary part in the coupling term. The results are summarized and discussed in the last section.

2 Basic equations

2.1 The Hamiltonian of an open quantum system

Let us consider the Hamilton operator

$$H = H_0 + \hat{V} \tag{1}$$

of a many-particle system where H_0 describes the mean-field, i.e. the motion of the particles in a finite depth potential and \hat{V} is the operator of the two-particle residual interaction. A convenient method to solve the Schrödinger equation $(H - E)\Psi = 0$ in the full Hilbert space of discrete and continuous states is to use the projection operator technique introduced by Feshbach [12]. Here the whole function space is divided into two subspaces by using the projection operators

$$\hat{Q} = \sum_{k=1}^{M} |\Phi_k\rangle\langle\Phi_k|$$

$$\hat{P} = \sum_{c} \int_{E_c}^{\infty} dE' |\xi_c(E')\rangle\langle\xi_c(E')|$$
(2)

with $\hat{P} + \hat{Q} = 1$, where Q contains the many-particle discrete states $|\Phi_k\rangle$ being solutions of $(\hat{Q}H\hat{Q} - E_k) |\Phi_k\rangle = 0$, and P the many-particle scattering states $|\xi_c(E)\rangle$ being solutions of

 $(\hat{P}H\hat{P}-E)|\xi_c(E)\rangle=0$. The total Hamiltonian acting on the full Hilbertspace is split into four terms: $H=\hat{Q}H\hat{Q}+\hat{Q}H\hat{P}+\hat{P}H\hat{Q}+\hat{P}H\hat{P}$.

We are interested in the properties of the Hamiltonian of the open quantum system, which acts on the Q subspace and carries the influence of the P space. The derivation of this Hamilton operator can be found in [1, 13],

$$H_{QQ}^{\text{eff}}(E) = \hat{Q}H\hat{Q} + \hat{Q}H\hat{P} \cdot G_P^{(+)}(E) \cdot \hat{P}H\hat{Q}.$$
(3)

It consists of two terms. The first one $(\hat{Q}H\hat{Q})$ describes the behaviour of the closed system of discrete states which includes the configurational mixing due to the two body residual interaction, but does not take into account the coupling to the decay channels. The second term gives the correction due to the coupling of the two subspaces and contains the propagator in the P-subspace $G_P^{(+)}(E) = \hat{P}[E + i\eta - \hat{P}H\hat{P}]^{-1}\hat{P}$.

Due to this propagator the effective Hamiltonian is energy dependent and non-hermitian. Its complex eigenvalues $\lambda_k(E) = \mathcal{E}_k(E) - i/2 \Gamma_k(E)$ give the poles of the resonance part of the scattering matrix

$$S_{cc'}^{\text{res}} = i \sum_{k=1}^{M} \frac{\gamma_{kc}(E)\gamma_{kc'}(E)}{E - \lambda_k(E)}$$

$$\tag{4}$$

where $\gamma_{kc}(E) = 1/\sqrt{2\pi} \langle \xi_c(E)|\hat{V}|\Phi_k\rangle$ is the transition matrix element between a bound and a scattering state. Thereby, the complex eigenvalues λ_k get a concrete physical interpretation as the energy positions $\mathcal{E}_k^{\text{res}} = \mathcal{E}_k(\mathcal{E}_k^{\text{res}})$ and total decay widths $\Gamma_k^{\text{res}} = \Gamma_k(\mathcal{E}_k^{\text{res}})$ of a resonance state [1, 13]. The \mathcal{E}_k differ usually from the corresponding eigenvalues E_k of $\mathcal{H}^0 \equiv \hat{Q}H\hat{Q}$, i.e. from the energies of the states of the unperturbed system. So the external coupling to the decay channels causes not only the finite lifetime of the states but generally also an energy shift.

In the following, we will restrict ourselves to an energy region in which the energy dependence of the Hamiltonian is small in spite of a large number M of states lying in it. Further, we consider a small number K of decay channels which are all open and not coupled among themselves. Then, the effective Hamiltonian (3) in the Q subspace is, to a good approximation,

$$\mathcal{H} = \mathcal{H}^0 - i\alpha V V^+ \tag{5}$$

where VV^+ is a hermitian operator if we consider time reversal invariance. As in Eq. (3) the first term \mathcal{H}^0 describes the internal structure of the unperturbed system in the Q subspace. The second term $i\alpha VV^+$ follows from $\hat{Q}H\hat{P}\cdot G_P^{(+)}(E)\cdot\hat{P}H\hat{Q}$ and describes the coupling between the two subspaces. The parameter α , assumed mostly to be real, characterizes the mean coupling strength between discrete and continuous states.

The Hamiltonian (5) is used successfully for the description of resonance states in nuclei [13] and molecules [9]. Nowadays, it is applied also to the description of resonance phenomena in other systems such as e.g. quantum dots [10] and microwave billards [11].

The rank of \mathcal{H}^0 is equal to the number M of states considered. Its non-diagonal matrix elements describe the configurational mixing of the discrete states. The coupling matrix V is a $K \times M$ matrix if the number of open decay channels is equal to K. The element V_i^c of V

describes the coupling of the discrete state i to the channel c; i = 1, ..., M; c = 1, ..., K. Thus, the rank of VV^+ is K.

As long as α is small, the second term of the Hamiltonian \mathcal{H} can be considered as a small perturbation of \mathcal{H}^0 . This condition is always fulfilled if the average width $\bar{\Gamma}$ is much smaller than the average distance \bar{D} between neighbouring resonance states. In this case, the non-diagonal matrix elements of \mathcal{H} are small, the individual resonances are isolated. Their positions and widths obtained from the eigenvalues λ_i of \mathcal{H} differ only slightly from the real and imaginary parts, respectively, of the diagonal matrix elements of \mathcal{H} .

In the opposite case of large α , the matrix VV^+ determines the behaviour of the system. Then, the rank of \mathcal{H} is given by K. That means, M-K states are almost decoupled from the continuum of decay channels and become long lived (trapped) while K states take almost the whole coupling strength: $\sum_{i=1}^K \Gamma_i/2 \approx \Im\{Tr(\mathcal{H})\}\$ and $\sum_{i=K+1}^N \Gamma_i \approx 0$. Therefore, two different time scales arise at large α , see e.g. [1, 2, 4, 5, 9].

Thus, a reorganization in the open quantum system takes place in the transition from small coupling parameters α to large ones when $M \gg K$. In the following, we will investigate the question whether and under which conditions the reorganisation of the open quantum system can be understood as a phase transition in the limit $M \to \infty$. We restrict ourselves to the case with one open decay channel (K = 1).

2.2The characteristic polynomial

We consider a system with M = 2N + 1 states coupled to one common decay channel (K = 1). The unperturbed eigenvalues of \mathcal{H}^0 are denoted by E_k , $k \in \{-N,...,N\}$, so that $E_j < E_k$ if j < k (without degeneration). The centre of the spectrum is assumed to be at $E_0 = 0$ without loss of generality. The coupling vector will be denoted by $V = (v_{-N}, ..., v_{-1}, v_0, v_1, ..., v_N)$.

Due to K=1, all column and row vectors, respectively, of VV^+ are linearly dependent. Substracting v_k times the row 0 from the row k, one gets the following expression for the characteristic polynomial,

$$P_{N}(\lambda) = \begin{vmatrix} E_{-N} - \lambda & 0 & 0 & \dots & \lambda v_{-N} & 0 & \dots & 0 \\ 0 & E_{-N+1} - \lambda & 0 & \dots & \lambda v_{-N+1} & 0 & \dots & 0 \\ \vdots & & \ddots & & \vdots & & \vdots & & \vdots \\ 0 & \dots & 0 & E_{-1} - \lambda & \lambda v_{-1} & 0 & \dots & 0 \\ -i\alpha v_{-N} & -i\alpha v_{-N+1} & \dots & -i\alpha v_{-1} & -i\alpha v_{0} - \lambda & -i\alpha v_{1} & \dots & -i\alpha v_{N} \\ 0 & & \dots & \lambda v_{1} & E_{1} - \lambda & \dots & 0 \\ \vdots & & & \dots & \lambda v_{N} & 0 & \dots & E_{N} - \lambda \end{vmatrix} = 0$$
ich can be written as

which can be written as

$$P_N(\lambda) = \prod_{k=-N}^{N} (E_k - \lambda) - i\alpha \cdot \sum_{k=-N}^{N} |v_k|^2 \cdot \prod_{j=-N, j \neq k}^{N} (E_j - \lambda) = 0.$$
 (6)

Eq. (6) can be proven by induction.

According to Eq. (6), $P_N(\lambda)$ is the sum of two polynomials,

$$P_N(\lambda) = Q_N(\lambda) - i\alpha \cdot R_N(\lambda), \tag{7}$$

where Q_N is of the order 2N + 1 and R_N of the order 2N. If $|v_k|^2 = 1 \quad \forall k$, the Q_N and R_N are related in a simple manner,

$$R_N = -\frac{d}{d\lambda}Q_N \ . \tag{8}$$

In the limit $\alpha = 0$, we find $\lambda_k = \mathcal{E}_k = E_k \ \forall k$, i.e. the eigenvalues of \mathcal{H} are equal to those of \mathcal{H}^0 (according to the definition of the parameter α).

The limit of large coupling strength $(\alpha \to \infty)$ can be obtained when we rewrite the characteristic polynomial (6) as

$$P_N(\lambda) = i\alpha \prod_{k=-N}^{N} (E_k - \lambda) \left[\frac{1}{i\alpha} - \sum_{j=-N}^{N} |v_j|^2 \frac{1}{E_j - \lambda} \right]. \tag{9}$$

The first factor of the product term is zero only at the unperturbed eigenvalues E_k of \mathcal{H}^0 . Therefore, for $\alpha \neq 0$ the solutions of Eq. (9) must be given by the zeros of the second factor, i.e. by the solutions of $\frac{1}{i\alpha} = \sum |v_k|^2 \frac{1}{E_j - \lambda}$. In the limit $\alpha \to \infty$, there are 2N solutions lying at real energies: $\lambda_k \in (E_k, E_{k-1})$ if k > 0 and $\lambda_k \in (E_k, E_{k+1})$ if k < 0 where E_k is eigenvalue of the unperturbed Hamiltonian \mathcal{H}^0 . In the case of the picket fence with $E_k = k$ and equal coupling, λ_k approaches $k \pm 1/2$. Furthermore, we have exactly one complex solution at $E_0 = 0$ and $\Gamma_0 \to \infty$ for $\alpha \to \infty$.

Let us now discuss the behaviour of the system as a function of increasing coupling strength α . From Eq. (7), we get

$$\frac{d\lambda}{d\alpha}Q_N'(\lambda) - iR_N(\lambda) - i\alpha\frac{d\lambda}{d\alpha}R_N'(\lambda) = 0$$
(10)

for the solutions of $P_N(\lambda) = 0$ and further the differential equation

$$\frac{d\lambda}{d\alpha} = \frac{iR_N(\lambda)}{Q_N'(\lambda) - i\alpha R_N'(\lambda)} \tag{11}$$

with the initial condition $\lambda_k(\alpha=0)=E_k$.

For small α , Eq. (11) reads

$$\frac{d\lambda_k}{d\alpha} \approx \frac{iR_N(\lambda_k)}{Q_N'(\lambda_k)} = -i|v_k|^2. \tag{12}$$

That means, the imaginary part of eigenvalue λ_k of \mathcal{H} increases, with increasing α , proportional to $|v_k|^2$ while the real part of it remains unchanged, as long as α is small.

For large α , we have 2N solutions whose imaginary part is small while the real part \mathcal{E}_k is determined by $E_k < \mathcal{E}_k < E_{k-1}$ if k > 0 and $E_k < \mathcal{E}_k < E_{k+1}$ if k < 0, since $\lambda_k(\alpha \to \infty) = \mathcal{E}_k$.

The relevant part of $R_N(\lambda)$ for the solutions of $P_N(\lambda) = 0$ is therefore $T_N(\lambda) = \prod_{k=1}^{2N} (\mathcal{E}_k - \lambda)$. Inserting

$$\lambda_k(\alpha) = \mathcal{E}_k - i\frac{g_k}{\alpha} + O(\alpha^{-2}). \tag{13}$$

into

$$0 = Q_N(\lambda) - i\alpha T_N(\lambda) \tag{14}$$

leads in the two lowest orders in $1/\alpha$ to

$$0 = \prod_{j=-N}^{N} (E_j + i\frac{g_k}{\alpha} - \mathcal{E}_k) - i\alpha \prod_{j=-N}^{2N} (\mathcal{E}_j - \mathcal{E}_k + ig_k/\alpha) . \tag{15}$$

The solution is

$$g_k = -\frac{\prod_{j=-N}^{N} (E_j - \mathcal{E}_k)}{\prod_{j=1, j \neq k}^{2N} (\mathcal{E}_j - \mathcal{E}_k)} > 0.$$
 (16)

Eq. (15) shows that for large coupling strengths, the decay widths of 2N states decrease as $\frac{1}{\alpha}$ with increasing α . This decrease is called resonance trapping.

Besides these 2N solutions for large α , we have a solution at $E_0 = 0$ and $\Gamma_0 \to \infty$ in the limit $N \to \infty$.

In sections 3 and 4, we will study in detail the properties of the characteristic polynomial (6) by means of special cases.

2.3 The eigenfunctions of a non-hermitian Hamilton operator

Another value characterizing the reorganization which takes place in the open quantum system under critical conditions, is the mixing of the wavefunctions of the resonance states [1, 4]. The mixing caused by the coupling of all the states to the common decay channels is related, in a natural manner, to the basic set of wavefunctions of the closed system,

$$\Phi_i = \sum_{i=1}^M a_{ij} \Phi_j^0 \tag{17}$$

where Φ_i are eigenfunctions of \mathcal{H} and Φ_j^0 are eigenfunctions of \mathcal{H}^0 . The eigenfunctions Φ_i of the non-hermitian Hamiltonian \mathcal{H} are bi-orthogonal. The right and left eigenfunctions are defined by

$$(\mathcal{H} - \lambda_i)|\Phi_i^r\rangle = 0$$

$$\langle \Phi_i^l|(\mathcal{H} - \lambda_i) = 0$$
(18)

with the normalization

$$\langle \Phi_i^l | \Phi_i^r \rangle = \delta_{i,j}, \quad \langle \Phi_i^r | \Phi_i^r \rangle \neq \delta_{i,j}$$
 (19)

In our case $|\Phi_i^l\rangle = (|\Phi_i^r\rangle)^T$ [5]. In the following we will drop the indices r and l considering only the right eigenfunctions. Then the second relation of Eq. (19) reads

$$\langle \Phi_i | \Phi_i \rangle \ge 1 \tag{20}$$

and $\langle \Phi_i | \Phi_j \rangle$, $i \neq j$, is a complex number, generally.

A good numerical measure for the strength of mixing is the number N_i^p of principal components in the eigenfunction Φ_i . For its definition we are using the quantity

$$b_{ij} = \frac{a_{ij}}{\sum_{l=1}^{M} |a_{il}|^2} \,. \tag{21}$$

Then, the number of principal components can be calculated as

$$N_i^p = \frac{1}{M \sum_{i=1}^M |b_{ij}|^4} \,. \tag{22}$$

The value of N_i^p can be understood as a measure of (external) collectivity of the resonance state Φ_i . In the limiting case of equal mixing of the state i with all states j, $b_{ij} = 1/\sqrt{M} \quad \forall j$, we get $N_i^p = 1$ (maximum external collectivity). In the opposite case (no external collectivity) we have $b_{ij} = \delta_{i,j}$ and $N_i^p = 1/M$. Generally, $1/M \leq N_i^p \leq 1$.

Further, we introduce the value

$$B = \frac{1}{M} \sum_{i=1}^{M} \langle \Phi_i | \Phi_i \rangle \ge 1 \tag{23}$$

which characterizes the degree of non-Hermiticity of \mathcal{H} according to Eq. (20). It is a function of α and B = 1 if \mathcal{H} is hermitian.

3 The ideal picket-fence distribution

Let us consider first the simple case of a picket-fence distribution of M=2N+1 levels which are all coupled with the same strength ("ideal picket-fence distribution") to the continuum consisting of one decay channel (K=1). The advantage of this simple model is that analytical studies can be performed.

3.1 Analytical study for the limiting case $N \to \infty$

Suppose $E_k = k$ und $|v_k| = 1 \quad \forall k$. Then Eq. (6) reads

$$P_N(\lambda) \equiv Q_N(\lambda) - i\alpha \cdot R_N(\lambda)$$

$$= \prod_{k=-N}^{N} (k-\lambda) - i\alpha \cdot \sum_{k=-N}^{N} \prod_{j=-N, j\neq k}^{N} (j-\lambda)$$
(24)

and the relation (8) holds. In order to consider the limit $N \to \infty$, we divide Q_N by a convergence ensuring factor,

$$\lim_{N \to \infty} \frac{Q_N(\lambda)}{-\prod_{k=1}^N - (k)^2} = \lim_{N \to \infty} \lambda \cdot \prod_{k=1}^N (1 - \frac{\lambda}{k})(1 + \frac{\lambda}{k}) = \lambda \cdot \prod_{k=1}^N (1 - (\frac{\lambda}{k})^2) = \frac{\sin(\pi \lambda)}{\pi}$$
(25)

Then the characteristic polynomial reads

$$P(\lambda) = \sin(\pi\lambda) + i\pi\alpha\cos(\pi\lambda) = 0.$$
 (26)

Denoting the complex eigenvalue of \mathcal{H} by $\lambda = \mathcal{E} - i\frac{\Gamma}{2}$ and splitting Eq. (26) into its real and imaginary part we get (for real α):

$$\cos(\pi \mathcal{E}) \left[e^{\pi \Gamma} (1 - \pi \alpha) - (1 + \alpha \pi) \right] = 0$$

$$\sin(\pi \mathcal{E}) \left[e^{\pi \Gamma} (1 - \pi \alpha) + (1 + \alpha \pi) \right] = 0$$
(27)

Since the two functions $\cos(x)$ and $\sin(x)$ never vanish for the same argument x, we have to consider two different cases:

1. $\sin(\pi \mathcal{E}) = 0 \Rightarrow \mathcal{E} = n \in \mathbb{Z}$ and

$$e^{\pi\Gamma} = \frac{1 + \pi\alpha}{1 - \pi\alpha} \tag{28}$$

has a real solution Γ for $\alpha < \frac{1}{\pi}$ only. For small α , we have therefore

$$\Gamma = \frac{1}{\pi} \ln \left(\frac{1 + \pi \alpha}{1 - \pi \alpha} \right) \tag{29}$$

and $\Gamma \to -\frac{1}{\pi} \ln \varepsilon$ for $\alpha = \frac{1}{\pi}(1-\varepsilon)$ and $\varepsilon \to 0$.

2. $\cos(\pi \mathcal{E}) = 0 \Rightarrow \mathcal{E} = n + \frac{1}{2} \text{ for } n \in \mathbb{Z} \text{ and }$

$$e^{\pi\Gamma} = \frac{\pi\alpha + 1}{\pi\alpha - 1} \,. \tag{30}$$

The last equation can be fulfilled only for $\alpha > \frac{1}{\pi}$. For large α it is therefore

$$\Gamma = \frac{1}{\pi} \ln \left(\frac{\pi \alpha + 1}{\pi \alpha - 1} \right) \tag{31}$$

and $\Gamma \to -\frac{1}{\pi} \ln \varepsilon$ for $\alpha = \frac{1}{\pi}(1+\varepsilon)$ and $\varepsilon \to 0$.

As a result: The widths of all the states increase up to infinity as a function of increasing α . The singularity at the critical point α_{crit} is determined by $\ln(\varepsilon)$. It is *logarithmic*.

Further, the energetical positions of the states remain unchanged at the unperturbed energies $E_k = k$ of the system (eigenvalues of \mathcal{H}_0) up to $\alpha \to \frac{1}{\pi}$. At $\alpha_{\text{crit}} = \frac{1}{\pi}$, the real part \mathcal{E}_k of 2N eigenvalues (all $k \neq 0$) of \mathcal{H} jumps from k to $k - \frac{1}{2}$ if k > 0 and from k to $k + \frac{1}{2}$ if k < 0, respectively. As a function of further increasing α , the imaginary part of the eigenvalues of the 2N resonance states (all k but k = 0) decreases first as $\ln(\alpha)$ while it approaches zero as $\frac{1}{\alpha}$ for $\alpha \to \infty$ according to Eq. (9).

In order to study the behaviour of the state in the centre of the spectrum at the energy $\mathcal{E}_0 = 0$ we consider only the highest-order terms of λ in Eq. (6):

$$\lambda^{2N+1} + i\alpha(2N+1)\lambda^{2N} = 0. (32)$$

For large α ($\alpha \gg \frac{1}{\pi}$), the state corresponding to the solution $\lambda = -i\alpha(2N+1)$ lies at $\mathcal{E} = 0$ and its width increases linear with α .

Summarizing the results, we state the following: In spite of the fact, that the coupling parameter α enters the equations (5) and (7) linearly, the imaginary parts of the complex eigenvalues show a singularity at the finite value $\alpha = \frac{1}{\pi}$. For larger couplings, a clear separation of the time scales with respect to the decay widths of the resonance states occurs. This happens also in the case of an infinitely extended spectrum. This is not a local effect of a *locally* broad resonance in a restricted energy region, but it is produced by the whole system in a *collective* manner. All basic states, independent of their energy position, act cooperatively.

3.2 Widths at the critical point for finite N: analytical study

The sum of the widths of all states is, in our simple example with equal coupling strengths, given by

$$\Im\{Tr(\mathcal{H})\} = \sum_{j} \frac{\Gamma_{j}}{2} = \alpha(2N+1) . \tag{33}$$

It is $Tr(\mathcal{H}) = \text{const }(\alpha)$. Thus, $\Im\{Tr(\mathcal{H})\}$ should be a smooth function of α not only far from the critical point but also near to it in spite of the divergence of the widths for $N \to \infty$ at $\alpha = \frac{1}{\pi}$ (see subsection 3.1). In the following, we will proof this statement.

First, let us consider the eigenvalues of \mathcal{H} for finite N. In this case, we have

$$P_N(\lambda) = \prod_{k=-N}^{N} (k - \lambda) \left[1 - i\alpha \sum_{j=-N}^{N} \frac{1}{j - \lambda} \right] = 0$$
 (34)

instead of the simple Eq. (26) holding for $N\to\infty$. As discussed in relation with Eq. (9), the solutions of $P_N(\lambda)=0$ follow from $1-i\alpha\sum_{j=-N}^N\frac{1}{j-\lambda}=0$. Here, we are interested in the difference between the solutions obtained for finite N and those for $N\to\infty$

It holds

$$0 = 1 - i\alpha \sum_{k=-N}^{N} \frac{1}{k-\lambda} = 1 + i\alpha\pi \cot(\pi\lambda) + 2i\alpha\lambda \sum_{k=N+1}^{\infty} \frac{1}{k^2 - \lambda^2}$$
 (35)

where the correction term is given by

$$2\lambda \sum_{k=N+1}^{\infty} \frac{1}{k^2 - \lambda^2} \approx 2\lambda \int_{N+1/2}^{\infty} \frac{dx}{x^2 - \lambda^2} = 2\int_{\frac{N}{\lambda}}^{\infty} \frac{dy}{y^2 - 1}$$

$$= \left[\ln \frac{y - 1}{y + 1} \right]_{\frac{N}{\lambda}}^{\infty} = \left[\ln \frac{1 - 1/y}{1 + 1/y} \right]_{\frac{N}{\lambda}}^{\infty}$$

$$= \left[\ln (1 - \frac{2}{y} + O(y^2)) \right]_{\frac{N}{\lambda}}^{\infty} \approx \left[-\frac{2}{y} \right]_{\frac{N}{\lambda}}^{\infty} = \frac{2\lambda}{N}$$
(36)

under the assumption $1/y = \lambda/N \ll 1$. This condition is fulfilled, to a good approximation, in the centre of the spectrum. Splitting Eq. (35) into its real and imaginary parts (with $\lambda = \mathcal{E} - \frac{i}{2}\Gamma$),

one arrives at

$$0 = 1 - \alpha \pi \frac{\sinh(\pi \Gamma)}{\cosh(\pi \Gamma) - \cos(2\pi \mathcal{E})} + \alpha \frac{\Gamma}{N}$$
(37)

for the real part. Here the identity

$$\cot(x+iy) = \frac{\sinh(2x) - i\sin(2y)}{\cosh(2y) - \cos(2x)}$$
(38)

is used. The equation for the imaginary part $(\mathcal{E} \neq 0)$ reads

$$0 = \alpha \pi \frac{\sin(2\pi \mathcal{E})}{\cosh(\pi \Gamma) - \cos(2\pi \mathcal{E})} + \frac{2\alpha \mathcal{E}}{N}$$
 (39)

from which we get

$$0 = \sin(2\pi\mathcal{E}) + \frac{2\mathcal{E}}{\pi N} \cosh(\pi\Gamma) - \frac{2\mathcal{E}}{\pi N} \cos(2\pi\mathcal{E}). \tag{40}$$

An estimation for the upper limit of the widths Γ of the states at $\alpha = \frac{1}{\pi}$ leads to

$$\pi\Gamma = \operatorname{arcosh}\left[\cos(2\pi\mathcal{E}) - \frac{N\pi}{2\mathcal{E}}\sin(2\pi\mathcal{E})\right] \approx \ln\frac{N\pi}{|\mathcal{E}|}.$$
 (41)

Here, we have used $N/|\mathcal{E}| \gg 1$ which is fulfilled only in the centre of the spectrum. Thus,

$$\frac{\Gamma}{2}(\alpha = \alpha_{\text{crit}}) \leq \frac{1}{2\pi} \ln \frac{N\pi}{|\mathcal{E}|}$$
(42)

which holds for every one of the 2N states (for all k but k=0) at the critical point. It means, $\Gamma \leq \ln N$ for $\alpha \to \frac{1}{\pi}$ for all N.

Using Eq. (42), one gets the following estimation for the trace of the imaginary part of H_{QQ}^{eff} at $\alpha = \frac{1}{\pi}$:

$$\sum_{j=-N}^{N} \frac{\Gamma_{j}}{2} \approx 2 \int_{0}^{N} dE \frac{1}{2\pi} \ln \frac{N\pi}{E} = -N \int_{0}^{1/\pi} \ln(x) dx = -N \left[x \ln(x) - x \right]_{0}^{1/\pi}$$

$$= \frac{N}{\pi} (1 - \ln \frac{1}{\pi}) = \frac{N}{\pi} (1 + \ln(\pi)) \approx \frac{2N}{\pi} \approx \frac{2N + 1}{\pi}. \tag{43}$$

The comparison of Eqs. (33) and (43) shows that Eq. (33) holds also at the critical point. This means, the singularity of the decay widths Γ at the critical point occurs such that the sum rule $\sum_i \Gamma_i = \operatorname{const}(\alpha)$ is fullfilled also for $\alpha \to \alpha_{\operatorname{crit}}$ and $N \to \infty$.

At the critical point, the width Γ_0 of the state in the centre of the spectrum can be estimated in leading order in N by integrating Eqs. (41) over the interval (-1/2, 1/2):

$$\frac{\Gamma_0}{2}(\alpha = \alpha_{\text{crit}}) = \frac{1}{2\pi} \int_{-1/2}^{1/2} \ln\left(\frac{N\pi}{|E|}\right) dE = \frac{1}{2\pi} (1 + \ln(2\pi N)) . \tag{44}$$

Thus, the width of the broadest state at the critical point is small in comparison to the total length 2N of the spectrum.

3.3 Numerical illustration

In the following, we illustrate the behaviour of the decay widths by results of numerical studies for different α and for some finite values of N between 50 and 5000.

Splitting the sum for finite N in Eq. (35) into its real and imaginary part, one gets

$$0 = \sum_{k=-N}^{N} \frac{k - \mathcal{E}}{(k - \mathcal{E})^2 + (\Gamma/2)^2}$$
 (45)

and

$$1 = \alpha \sum_{k=-N}^{N} \frac{\Gamma/2}{(k-\mathcal{E})^2 + (\Gamma/2)^2} . \tag{46}$$

The first equation describes the trajectories of the eigenvalues $\lambda = \mathcal{E} - \frac{i}{2}\Gamma$ of \mathcal{H} in the complex plane while the second one contains their parametrization with α . We calculated the sum in Eq. (45) for different N and fixed values of Γ and traced their solutions as a function of \mathcal{E} .

In Fig. 1.a, the results of the calculations for different N (N=500,1000,5000) and fixed $\Gamma=1$ are shown as a function of \mathcal{E} . Due to the denominator of the sum, every resonance state k with $\Gamma_k \geq 1$ has two solutions while there are no solutions when $\Gamma_k < 1$. The number of solutions and thus the number of resonance states with $\Gamma_k > 1$ depends on the average slope by which the sum approaches the value 0 as a function of \mathcal{E} .

The result is as follows: For a fixed value of $\Gamma = 1$ there are the more solutions of Eq. (45), the larger N. In the limit $N \to \infty$, Eq. (45) can be fulfilled for all resonances, i.e. all resonance states have widths larger than an arbitrarily chosen finite value. This confirms the analytical result for an infinite number of states, where we have shown that the widths of *all* states diverge at $\alpha = \alpha_{\rm crit}$.

In Fig. 1.b, the results of calculations are shown with a fixed number N=1000 and different values of Γ ($\Gamma=0.5, 0.75, 1.0$). In this case, the average slope of the different curves is the same but the amplitude of the oscillations varies. The larger Γ the smaller the amplitude is. That means, in the case of finite N, the number of resonance states having $\Gamma_k \geq \Gamma$ is the smaller the larger Γ .

As a result, we state the following: When N is a finite number, only a limited number of resonance states has widths $\Gamma_k \geq \Gamma$ where Γ is an arbitrarily chosen finite value. Further, the larger N, the larger the number of resonance states with $\Gamma_k \geq \Gamma$. On the other hand, the larger Γ , the smaller the number of resonance states with $\Gamma_k \geq \Gamma$. Thus we have two processes compensating each other which ensures, that (33) holds also in the limit $\alpha \to \frac{1}{\pi}$ and $N \to \infty$.

In Fig. 2.a, we illustrate the motion of the eigenvalues in the complex plane for $0.01 < \alpha < 2$ in steps of 0.01 for positive energy \mathcal{E} (the part for negative energy is symmetric to that for positive energy). For each resonance state its eigenvalue follows a certain trajectory with increasing α . For the lowest values of α , all eigenvalues are near to $E_k = k$ and $\Gamma_k/2 = \alpha$. The full line gives the estimation for the upper limit of $\Gamma/2$ at $\alpha = \alpha_{\rm crit}$ according to Eq. (42). The estimation is good in the centre of the spectrum. The deviations at large energies are pure boundary

effects. The differences between the different eigenvalue trajectories arise from the finite value of N. In the limit of $N \to \infty$ all eigenvalues acquire the same behaviour because of the discrete translational symmetry on the real energy axis.

We show in Fig. 2.b the behaviour of all $\Gamma_k/2$ as a function of α for N=50. At the critical value $\alpha_{\rm crit}=1/\pi$ (indicated by a vertical solid line) the width of the collective resonance state k=0 separates from the widths of the other ones and increases linearly. The slope of $\Gamma_0(\alpha)/2$ is equal to 2N+1 over almost the whole range of $\alpha>\alpha_{\rm crit}$ according to Eq. (32). The larger slope of $\Gamma_0(\alpha)$ close to $\alpha_{\rm crit}$ is a boundary effect and disappears in the limit of $N\to\infty$.

Fig. 2.c shows N_0^p as a function of α for two different values of N. The curves show a sudden rise at α_{crit} and saturate rapidly to 1. The inlet gives a magnification of the curve around the critical point which is marked by a vertical solid line. The larger N, the sharper are the changes in the slope of $N_0^p(\alpha)$. This is a clear numerical indication of the cooperative effect acting over the total length of the spectrum. In spite of the fact, that the width Γ_0 of the fast decaying state at $\alpha \approx \alpha_{\text{crit}}$ is of the order $\ln(M)$, eq. (44), its wavefunction carries contributions from basis states which are lying far away from the centre of the spectrum and are not overlapped by it. These contributions over large energy scales are achieved via the "chain" of overlapping neighbouring resonances. As a result, we observe a "macroscopic" order over the whole energy scale of the system being much larger than Γ_0 .

The curve of N_0^p does, of course, not jump immediately to 100% at the critical point. The main reason is the finite number of states taken into account in the calculations. The widths of the resonances at the border of the spectrum are in general smaller than those of the resonances inside the spectrum. Therefore the chain of neighbouring overlapping states is interrupted at energies close to the edges.

For all the trapped states the corresponding quantity N_k^p always remains in the order of 1/M. The wavefunctions of these states are mixed only with those of their next neighbours.

All the numerical results show that although the phase transition appears mathematically for $N \to \infty$ only, the characteristic features of it can be already seen at *comparably* small values of M.

3.4 Picket-fence level distribution with disturbed translation invariance

Let us break the translation invariance of the picket-fence model by giving another coupling strength to the state in the centre of the system. Suppose: $E_k = k$ und $|v_k| = 1 \quad \forall k - \{0\}$ and $v_0 = 1 + D$. In this case, the characteristic polynomial (6) reads

$$P_N(\lambda) = \prod_{k=-N}^{N} (k - \lambda) - i\alpha \sum_{k=-N}^{N} \prod_{j \neq k} (j - \lambda) - i\alpha D \prod_{k=1}^{N} (k - \lambda)(k + \lambda) . \tag{47}$$

Dividing by a convergence ensuring factor and identifying the resulting terms with the product representation of sin(x) and cos(x), respectively, we get

$$P(\lambda) = \frac{\sin(\pi\lambda)}{\pi} + i\alpha\cos(\pi\lambda) + i\alpha D \frac{\sin(\pi\lambda)}{\pi\lambda} = 0$$
 (48)

in the limiting case $N \to \infty$. In order to study the behaviour of the state in the centre $(\mathcal{E} = 0)$ we write $\lambda = -i\mu$ and get

$$\alpha = \frac{1}{\pi} \left[\frac{1}{\frac{D}{\pi\mu} + \coth(\pi\mu)} \right] . \tag{49}$$

According to this equation, $\alpha \to \frac{1}{\pi}$ for $\mu \to \infty$. The redistribution of the system takes place at the same finite value of $\alpha_{\rm crit} = 1/\pi$ as in the case of constant coupling.

We investigate now the behaviour of the system at the critical point, i.e. the type of the singularity. Suppose $\varepsilon = 1 - \pi \alpha$ and $\pi \mu = c \varepsilon^{-s}$ with $s \in R$. Using the relation $\coth(\pi \mu) \to 1$ for large μ , we get from (49)

$$1 = (1 - \varepsilon)(1 + \frac{D}{c}\varepsilon^{+s}). \tag{50}$$

In leading order of the singular part of $\pi\mu(\varepsilon)$, this equation is solved by s=1 and $c=D(1-\varepsilon)\approx D$. That means, we have an algebraic singularity: $(\pi\mu=\frac{D}{\varepsilon})$. The system approaches the singularity quicker than in the case of a picket fence with translation invariance.

In the following we like to discuss formula (49) in detail with the help of a numerical illustration (Figs. 3 and 4). It turned out, that the case with a discriminated state at $\mathcal{E} = 0$ is more complicated. Therefore we have drawn the movement of the complex eigenvalues λ in the centre of the spectrum for D = -0.5 (Fig. 3.a). We use M = 2N + 1 = 101 and 301, respectively.

At $\alpha = \alpha_{\rm crit} = 1/\pi$ two broad modes arise at the flanks of the spectrum at $|\mathcal{E}| \approx 4.5$ and 7.5 for N=50 and 150, respectively. The larger the number of resonance states is, the larger is their distance from the centre. With increasing α the poles of the two resonance states at positive and negative energy approach each other in their real part and collide at $\mathcal{E}=0$ at a certain value $\alpha=\alpha_{c1}$. At $\alpha>\alpha_{c1}$, the resonance states remain at $\mathcal{E}=0$, one with further increasing, the other one with decreasing Γ . The more resonance states the spectrum contains the smaller is α_{c1} , as one can see in Fig. 3.b. Here the imaginary parts $\Gamma_k/2$ of the eigenvalues λ_k shown in Fig. 3.a are drawn as a function of the coupling strength α . The collision point shifts to the critical point of the spectrum ($\alpha_{c1} \to \alpha_{\rm crit}$) if the number M of resonance states is enlarged, in spite of the fact that their distance from one another at α_{c1} is larger when M is larger. The two values of α_{c1} corresponding to M=101 and M=301, are indicated by vertical dashed lines. The values of $\alpha_{\rm crit}$ and α_{c2} are marked by vertical solid lines. In the limit $M\to\infty$ the two broad poles appear at $\mathcal{E}\to\infty$. In this limit, $\alpha_{c1}\to\alpha_{\rm crit}$. At this point of α , the poles jump to $\mathcal{E}=0$.

Between $\alpha = \alpha_{c1}$ and the finite value $\alpha = \alpha_{c2}$, there exist three resonance states at $\mathcal{E} = 0$: the two broader poles appearing at α_{c1} and the original one which is discriminated by the external coupling by D. The collective mode is one of the two resonance states arising from the phase transition at $\alpha = \alpha_{c1}$. Its imaginary part increases with further increasing α . The other broad pole decreases in Γ with increasing α . Its collision with the discriminated resonance state at $\alpha = \alpha_{c2}$ shifts both states away from $\mathcal{E} = 0$ and the imaginary part of both eigenvalues decreases. Contrary to the value of α_{c1} which approaches α_{crit} with $M \to \infty$ the value of α_{c2} remains almost constant as a function of M. For $M \to \infty$, the value of α_{c2} remains larger than α_{crit} . As we will see below, it mainly depends on D. The poles of the trapped states approach the values n + 1/2 (with $n \in \mathbb{Z}$) if $\alpha \to \infty$.

Figs. 4.a. and 4.b. show the graphs of $\pi\mu \coth(\pi\mu) + D$ for different D (D = -0.5, 0, 0.5) and μ/α for several values of α as a function of μ . The points of intersection are the solutions of equation (49) derived under the assumption of an infinite number of states.

In Fig. 4.a. the coupling parameter is set to $\alpha = 0.1 < \alpha_{\rm crit}$ and $\alpha = 1/\pi = \alpha_{\rm crit}$, respectively. For the value $\alpha < \alpha_{\rm crit}$ there exists only one point of intersection with each of the curves of coth, lying at small values of μ . Also the state at $\mathcal{E} = 0$ has a comparably small width in the undercritical regime of α and the value of μ increases with increasing D. In the parameter range $\alpha < \alpha_{\rm crit}$ no broad mode is separated from the other ones.

At the critical point $\alpha = \alpha_{\rm crit}$, where the phase transition takes place, the linear curve μ/α is tangential to the $\pi\mu \coth(\pi\mu) + D$ for D=0 and is parallel to this function for D=-0.5, 0.5 (lower and upper thick full line, respectively). So each of these curves has a point of intersection with μ/α at $\mu=\infty$. For the case D=-0.5, the intersection at $\mu=\infty$ contains two solutions for the two broad modes, arising at the borders (at $\mathcal{E}=\pm\infty$) of the spectrum and colliding at $\mathcal{E}=0$. Additionally, there is another intersection with μ/α at a small value of μ which arises from the discriminated state at $E_0=0$.

In Fig. 4.b, we see the same curves $\pi\mu \coth(\pi\mu) + D$ as in Fig. 4.a together with μ/α for different values of $\alpha > \alpha_{\rm crit}$: $\alpha < \alpha_{c2}$, $\alpha \approx \alpha_{c2}$ and $\alpha > \alpha_{c2}$. In all cases, the curves have intersections at $\mu = \infty$. This means, for all values of D a mode exists at $\mathcal{E} = 0$ with an infinitely large width if $\alpha \geq \alpha_{\rm crit}$. The curve $\pi\mu \, \coth(\pi\mu) - 0.5$ shows three intersections with μ/α in the range $\alpha_{\rm crit} < \alpha < \alpha_{c2}$. The two intersections at smaller μ approach each other if $\alpha \to \alpha_{c2}$. The value of α_{c2} depends obviously on the value of D. In dependence on the negative shift of $\coth(\pi\mu)$ the slope of the tangent changes and therefore the value of α_{c2} . At larger values of the coupling $(\alpha > \alpha_{c2})$ only one solution remains at $\mathcal{E} = 0$ with $\mu = \infty$.

Finally we have investigated the behaviour of the number N_0^p of principal components of the broad resonance as a function of α for $D=\pm 0.5$ and M=101 states. The results are drawn in Fig. 5 together with the former one for D=0. For all cases the sudden rise of N_0^p at $\alpha \approx \alpha_{\rm crit}$ can be seen. At the critical point the collective state is created, in all cases, by almost all basis states distributed over the whole spectrum. This collective behaviour of a phase transition is well pronounced also for $D \neq 0$. The curve for D=0.5 is, however, much smoother than the other ones. It rises up not as quickly as the other ones and does not approach the maximum value 100% in the range of α shown in the figure. Nevertheless, the characteristics of a phase transition can be seen also in this numerical study: Comparing the results for M=301 states in the case of D=0.5 with those for M=101 states we see the following tendency. By increasing the number of states, N_0^p for D=0.5 comes closer to the curves N_0^p for D=1 and -0.5. This behaviour is a hint to a phase transition (in the next section, Fig. 7.a, we show an example in which a phase transition does not occur and the results as a function of an increasing number M of states do not show such a tendency).

3.5 Phase transition

Summarizing the results of our study with the ideal picket fence, we state the following.

– For an infinite number of states the imaginary parts of the complex eigenvalues of the effective Hamiltonian (5) show a singularity at the finite value $\alpha = \alpha_{\rm crit} = 1/\pi$. A

bifurcation in the widths appears: the width $\Gamma_{i=0}$ of the state in the centre of the spectrum increases with further increasing α while the widths of all the other states start to decrease. All states but the state at E=0 are shifted by 1/2 at $\alpha=\alpha_{\rm crit}$. For finite M the width $\Gamma_{i=0}$ increases linearly with $\alpha>\alpha_{\rm crit}$ with a slope given by the number M of states included in the spectrum.

- The state in the centre of the spectrum is a collective one in a global sense. The numerical studies for finite systems show that it contains components of almost *all* basic states of the system, also of those which are *not* overlapped by it. This is expressed by the number $N_{i=0}^p$ of principal components of the state in the centre of the spectrum which grows, at $\alpha = \alpha_{\text{crit}}$, suddenly from its minimum value to 100% (maximum mixing).
- At $\alpha = \alpha_{\rm crit}$, the width $\Gamma_{i=0}$ of the state in the centre of the spectrum is much smaller than the extension of the spectrum. Therefore, the system does *not* create locally a collective state which traps, with increasing α , further resonance states overlapped by it.
- At $\alpha = \alpha_{\rm crit}$, the system suffers a change in its structure: one of the resonance states aligns with the decay channel. Its wavefunction collects all the corresponding components from the wavefunctions of all the other states (which appear with the same weight in all basic wavefunctions because of the symmetry of the problem). Therefore, its width $\Gamma_{i=0}$ increases with further increasing α while the widths of all the other states decrease.

Generally, the behaviour of the order parameter of a system as a function of a control parameter characterizes the type of the phase transition. In case of a first order phase transition the order parameter shows a jump at a certain finite value of the control parameter $\alpha = \alpha_{\rm crit}$. If a higher order phase transition is present, the corresponding derivative of the order parameter jumps at $\alpha_{\rm crit}$. More precicely, its (n-1)-th derivative jumps in case of an n-th order phase transition.

In our system, the value Γ_0/M can be understood as the order parameter. It is the width of the collective state normalized according to the number of resonance states contributing to its formation. This value increases linearly as a function of α with the slope 1/M for $\alpha < \alpha_{\rm crit}$ and with the slope one if $\alpha > \alpha_{\rm crit}$. So, the first derivative of Γ_0/M jumps at $\alpha = \alpha_{\rm crit}$. Therefore we conclude, that the formation of a globally collective resonance is a second order phase transition. We will prove in the next sections, that this behaviour is universal for all systems showing a collective reorganisation.

In sections 4.5 and 5, we will see that the phase transition is accompanied by an essential deviation of the value B (Eq. (23)) from 1 in the neighbourhood of $\alpha_{\rm crit}$. This means the bi-orthogonality of the function system plays an important role in the reordering process.

4 More realistic systems

In the previous section, we investigated the properties of the translation invariant picket-fence model as a function of the coupling parameter α analytically as well as numerically. The system suffers a second-order phase transition at $\alpha = \frac{1}{\pi}$ which we studied in detail. We consider now the behaviour of some more realistic systems as a function of the parameter α in order to answer the question whether the results obtained have a general meaning. In detail, energy dependencies

and fluctuations within the spectrum will be considered in the following.

4.1 System with unequally distributed levels and equal coupling strength

We investigate now the behaviour of systems when the level density is not constant but changes as a function of energy. Suppose: $E_k = \text{sign}(k) \ k^2 \ \text{und} \ v_k = 1 \quad \forall k$. This means, the level density is assumed to decrease linearly with k and to approach the value zero for $k \to \infty$.

In this case, the characteristic polynomial reads

$$P_N(\lambda) = \prod_{k=-N}^{N} \left(\operatorname{sign}(k) \ k^2 - \lambda \right) - i\alpha \sum_{k=-N}^{N} \prod_{j=-N; j \neq k}^{N} \left(\operatorname{sign}(j) \ j^2 - \lambda \right)$$
 (51)

which can be rewritten as

$$P_N(\lambda) = Q_N(\lambda) + i\alpha \cdot \frac{d}{d\lambda} Q_N(\lambda)$$
 (52)

where $Q_N(\lambda) = \prod_{k=-N}^N \left(\operatorname{sign}(k) \ k^2 - \lambda \right)$. Dividing $Q_N(\lambda)$ by the convergence ensuring factor $F = -\prod_{k=1}^N -(k)^4$ we get

$$\frac{Q_N(\lambda)}{F} = \lambda \prod_{k=1}^N \left(1 - \frac{\lambda}{k^2}\right) \left(1 + \frac{\lambda}{k^2}\right). \tag{53}$$

In the limit $N \to \infty$, this expression is

$$\frac{Q_N(\lambda)}{F} = \frac{1}{\pi^2} \sin(\pi\sqrt{\lambda}) \sinh(\pi\sqrt{\lambda}) = \frac{-i}{\pi^2} \sin(\pi\sqrt{\lambda}) \sin(i\pi\sqrt{\lambda})$$

$$= \frac{-i}{2\pi^2} \left[\cos(\pi\sqrt{\lambda}(1-i)) - \cos(\pi\sqrt{\lambda}(1+i)) \right] \tag{54}$$

according to the Weierstrass product representation. In order to find the solution at $\mathcal{E} = 0$, we write $\lambda = i\mu$ and get

$$\frac{Q_N(\lambda)}{F} = \frac{-i}{\pi^2} \left[\cos(\pi \sqrt{2\mu}) - \cosh(\pi \sqrt{2\mu}) \right]$$
 (55)

and finally, with $\frac{d}{d\lambda}Q_N = \frac{1}{i}\frac{dQ_N}{d\mu}$

$$\alpha = \frac{\sqrt{2\mu} \cosh(\pi \sqrt{2\mu}) - \cos(\pi \sqrt{2\mu})}{\pi \sinh(\pi \sqrt{2\mu}) + \sin(\pi \sqrt{2\mu})}.$$
 (56)

The right-hand side of this equation is a monotonically increasing function: $\alpha \to \infty$ with $\mu \to \infty$. The dilution of the spectrum at large $|\mathcal{E}|$ prevents therefore a phase transition.

Fig. 6.a shows $\Gamma_k/2$ as a function of α for N=50 states. A short-lived state is formed, but in contrast to the ideal picket fence (Fig. 2.b), no critical value of α can be defined. The width of the state in the centre of the spectrum (at $\mathcal{E}=0$) increases smoothly as a function of α trapping step by step its neighbours. The formation of the short-lived state does not occur by a collective interaction of all basis states but by individual trapping of neighboured levels. In other words, the short-lived state is not formed by a cooperative effect acting over the whole energy scale of the spectrum but is restricted to the energy range overlapped by it. There is no phase transition.

The number N_0^p of principal components in the wavefunction of the state k=0 is shown as a function of α in Fig. 7.a for N=50 and 150. It supports the conclusion drawn. Also this value is a smooth function. There is no hint to a phase transition. The broad state carries only components of those basis states which it overlaps. In contrast to the cases where a phase transition occurs, the slope of N_0^p decreases with increasing N. The curve N_0^p in Fig. 7.a remains smooth unlike the curves for D=0.5 and M=101,301 states in Fig. 5. The collective state is created by the basis states of a local energy region overlapped by it.

4.2 System with unequally distributed levels and unequal coupling strength

We investigate now the question whether a system with diluted level density at large $|\mathcal{E}|$ shows a phase transition if the states at the border are coupled stronger to the decay channel than those in the centre of the spectrum.

To this purpose we rewrite Eq. (9),

$$\alpha = \frac{-i}{-\frac{|v_0|^2}{\lambda} + \sum_{k=1}^{N} \left[\frac{|v_k|^2}{E_k - \lambda} + \frac{|v_{-k}|^2}{E_{-k} - \lambda} \right]}$$
 (57)

As in the foregoing examples, the spectrum is supposed to be symmetrical (or nearly symmetrical) in relation to $E_{k=0} = 0$: $-E_k \approx E_{-k}$ und $v_k \approx v_{-k}$. Looking at the solution at E = 0, we write $\lambda = -i\mu$. Then we get

$$\alpha \approx \frac{-1}{\frac{|v_0|^2}{\mu} + \sum_{k=1}^{N} \frac{2\mu |v_k|^2}{E_k^2 + \mu^2}}$$
 (58)

from Eq. (57). Since we are interested in the question whether the system shows a phase transition at a finite value of α , we have to consider (58) in the limiting case $\mu \to \infty$ and $N \to \infty$:

$$\frac{1}{\alpha_{\text{crit}}} = \lim_{\mu \to \infty} \left[\lim_{N \to \infty} 2\mu \sum_{k=1}^{N} \frac{|v_k|^2}{E_k^2 + \mu^2} \right] . \tag{59}$$

We approximate Eq. (59) by an integral, replace the discrete index k by the continuous variable x and assume $E_k^2 \approx x^t$ und $v_k^2 \approx x^r$. Then

$$\frac{1}{\alpha_{\text{crit}}} = \lim_{\mu \to \infty} 2\mu \int_0^\infty \frac{x^r}{x^t + \mu^2} dx = \lim_{\mu \to \infty} 2\mu^{2\frac{r+1}{t} - 1} \int_0^\infty \frac{s^r}{s^t + 1} ds . \tag{60}$$

The integral converges when $t = r + 1 + \varepsilon \ \forall \varepsilon > 0$.

Let us consider the following cases.

- 1. 2(r+1) > t. In this case, $\alpha_{\rm crit} \to 0$ with $\mu \to \infty$. The system is in an overcritical situation for all $\alpha > 0$. A phase transition does therefore not take place.
- 2. 2(r+1) = t. In this case, $\alpha = \alpha_{\rm crit} > 0$ remains finite in the limiting case $\mu \to \infty$. For $\alpha < \alpha_{\rm crit}$, the widths of all states increase. At $\alpha = \alpha_{\rm crit}$, a phase transition takes place: the short-lived state appears suddenly and a clear separation of time scales, with respect to the lifetimes of the resonance states arises, even if the spectrum is infinitely extended.

3. 2(r+1) < t. In this case, $\alpha_{\text{crit}} \to \infty$ with $\mu \to \infty$. For all finite values of α , there exist states which are not overlapped by the collective resonance, whose widths increase with increasing α . Therefore, the state at $\mathcal{E} = 0$ traps new states endlessly. As a consequence, the formation of the short-lived state at $\mathcal{E} = 0$ takes place smoothly. A phase transition does *not* take place.

This analytical study shows the following result. To fulfill the conditions for a phase transition, the energy dependence of the unperturbed spectra of \mathcal{H}^0 must be compensated by an energy dependent coupling of the individual states to the decay channel. A phase transition exists in the cases considered, if the energy dependence of the distribution of the levels E_k is opposite to that of the coupling matrix elements v_k . According to Eq. (60), the critical value of α is

$$\alpha_{\rm crit} = \frac{r+1}{\pi} = \frac{t}{2\pi} \ . \tag{61}$$

Otherwise, the system is either in an overcritical regime (corresponding to $\alpha_{\rm crit} \to 0$) or in an undercritical one (corresponding to $\alpha_{\rm crit} \to \infty$).

Further the width of the broad pole at $\alpha \approx \alpha_{\text{crit}}$ in the compensated case $(r \neq 0)$ can be estimated with respect to the length of the spectrum. The characteristic polynomial (Eq. (9)) at the energy of the collective state $(\mathcal{E} = 0)$ reads:

$$\frac{-i}{\alpha} = \sum_{k=-N}^{N} \frac{|v_k|^2}{E_k + \frac{i}{2}\Gamma} = \sum_{k=-N}^{N} \frac{|k|^r (k |k|^r - \frac{i}{2}\Gamma)}{(k^{r+1})^2 + \Gamma^2/4}$$
(62)

The principal value of that sum gives zero. Therefore we can write:

$$\frac{1}{\alpha} = \frac{\Gamma}{2} \sum_{k=-N}^{N} \frac{|k|^r}{(k^{r+1})^2 + \Gamma^2/4}$$

$$\approx \frac{\Gamma}{2} \int_{-N}^{N} \frac{|x|^r}{(x^{r+1})^2 + \Gamma^2/4} dx = \frac{\Gamma}{r+1} \int_{0}^{N^{r+1}} \frac{ds}{s^2 + \Gamma^2/4}$$

$$= \frac{2}{r+1} \int_{0}^{\frac{2N^{r+1}}{\Gamma}} \frac{d(\frac{2S}{\Gamma})}{(\frac{2S}{\Gamma})^2 + 1} = \frac{2}{r+1} \arctan\left(\frac{2N^{r+1}}{\Gamma}\right) \tag{63}$$

Using the expression (61) for the critical point of the infinite system one gets:

$$\frac{\pi}{2} \approx \arctan\left(\frac{2N^{r+1}}{\Gamma}\right)$$
 (64)

which holds only if $\Gamma \ll 2 \cdot N^{r+1}$. In other words, also in the compensated case, the width of the fast decaying collective resonance state is much smaller than the extension of the spectrum at a coupling strength close to the critical point.

The compensated case is illustrated in Figs. 6.b and 7.b, the overcompensated one in 6.c and 7.c. In the compensated case (with r=1), both the distance between neighbouring levels and the coupling strength $|v_k|^2$ increase linearly with |E|, $(E_k = \text{sign}(k) \ k^2 \text{ and } |v_k|^2 = |k| + 1 \ \forall k)$. In the overcompensated case, the energy dependence of the coupling is chosen stronger than the dilution of the spectrum $(E_k = \text{sign}(k) \ k^2 \text{ and } v_k = |k| + 1 \ \forall k)$. Here the coupling increases

quadratically whereas the level density decreases linear with E.

The compensation of the energy dependence of the level density by a corresponding one in the coupling strength restores the phase transition (Figs. 6.b and 7.b as compared with 6.a and 7.a). A collective mode is created by participation of (almost) all basis states. It occurs suddenly at a critical value of α .

In Fig. 7.b N_0^p for M=101,301 and 1001 states is drawn. With increasing number M of states the curve rises more and more sharply. The critical value is $\alpha_{\rm crit}=2/\pi$ (indicated by a vertical solid line) in accordance with Eq. (61).

The maximum value $N_0^p = 1$ is not reached in Fig. 7.b. N_0^p is approximately 0.9 and even decreases with further increasing α . Drawing the contributions b_{0i} in the wavefunction Φ_0 , Eq. (21), one sees the following feature. The contributions of the states j coupled more weakly to the channel decrease for $\alpha > \alpha_{\rm crit}$ in contrast to those of the states i coupled more strongly: $v_j < v_i \longrightarrow |b_{0j}| < |b_{0i}|$. Since the differences between the v_i are quite large in the cases considered, $N_0^p < 1$. This holds for both cases, decreasing and increasing energy dependence of the level density. In both cases, the coefficients $|b_{0j}|$ are spread at large α , e.g. at $\alpha \approx 4\alpha_{\rm crit}$. This is in contrast to the case of the ideal picket fence with equal coupling strengths, in which all coefficients approach the value 1/M for $\alpha \geq 2\alpha_{\rm crit}$.

In the case of an overcompensation (Fig. 6.c and 7.c) the critical point is shifted to very small values in accordance with $\alpha_{\rm crit} \to 0$, Eq. (60). The number of principal components of the broad mode jumps up to 75%. Then it decreases and saturates at around 57%.

In an additional calculation, we bounded the spectrum from below: we investigated the case with $E_k = k^2$, $|v_k|^2 = k + 1 \forall k$, $k \geq 0$. Also in this system, a phase transition takes place at $\alpha_{\rm crit} = 2/\pi$ as in the case shown in Figs. 6.b and 7.b. In all cases, the broad mode appears in the energetical centre of the spectrum.

4.3 System with unfolded Gaussian distributed levels

It is interesting to learn whether the conditions for a phase transition must be fulfilled strictly or only on the average. In order to answer this question in the affirmative, we perform the following numerical analysis. We choose an unfolded Gaussian-Orthogonal Ensemble (GOE) for the distribution of the eigenvalues of \mathcal{H}^0 and a Gaussian distributed coupling vector V with mean value $\langle v \rangle = 1$ and variance $\Delta v = 0.01$.

The decay widths as a function of the coupling parameter α are drawn in Fig. 6.d. for N=50. The broad mode separates from the other ones at approximately $\alpha_{\rm crit}=1/\pi$ with a slope of 2N+1. The features of the phase transition are not as clearly pronounced in this figure as in the case of the ideal picket fence. Nevertheless, the differences to Fig. 6.a., where no phase transition occurs, are obvious. Even for the comparably small number of states (M=101), the fluctuations in the distribution of the levels and the coupling vector do not destroy the nature of the reorganisation process.

As shown in the foregoing sections, the number of principal components N_k^p is a sensitive

quantity to measure the global collectivity of the separation process. In Fig. 7.d. N_0^p of the collective mode at E=0 is drawn as a function of α for N=50,150,250,500. For increasing M=2N+1 the curves rise up more suddenly and the slope near $\alpha=1/\pi$ gets steeper. All the curves approach the maximum value of N_0^p very fast for values $\alpha>\alpha_{\rm crit}$.

The features of the second-order phase transition are better expressed if more resonance states are considered. For large N the irregularities in the distribution of the E_k and v_k are almost unimportant. This proves, that the conditions derived in the former sections have to be fullfilled only on the average. Also in the ergodic case of a GOE distributed spectrum, the reorganisation of the spectrum can be understood as a second-order phase transition. The fluctuations within the spectrum will be washed out if the conditions for a phase transition derived from Eq. (60) are fulfilled on the average.

4.4 System with complex coupling parameter α

Up to now, we considered the system to be described by the Hamiltonian \mathcal{H} , Eq. (5), where the coupling between system and continuum is supposed to be real and \mathcal{H} is non-hermitian. There may be an additional part $\beta \tilde{V}\tilde{V}^+$ in the coupling term by which a collective state of another (internal) type is created. This collective state is shifted by an energy $\Delta \mathcal{E}$ from the group of the remaining N-1 states [6]. The structure of both parts VV^+ and $\tilde{V}\tilde{V}^+$ is the same. The difference is the non-hermiticity of the external coupling term in the first case and the hermiticity in the second case.

We are interested in the question whether the additional term has an influence on the phase transition. Investigating this question, we restrict ourselves to the case $VV^+ = \tilde{V}\tilde{V}^+$, i.e. an angle zero between the vectors V and \tilde{V} . Further, the characteristic polynomial (6) does not contain, in the one-channel case, the phases of the coupling matrix elements, but only $|v_k|^2$. It is justified, therefore, to replace α by $\alpha + i\beta$ in the equations considered in the previous sections in order to get conclusions on the influence of the term with $\beta \neq 0$ on the phase transition.

Considering the picket-fence model with equal coupling strength (which we studied in section 3 for $\beta = 0$) Eq. (26) must be replaced by

$$P(\lambda) = \sin(\pi\lambda) + i\pi(\alpha + i\beta)\cos(\pi\lambda) \tag{65}$$

Using the representation $\lambda = \mathcal{E} - \frac{i}{2}\Gamma$, one gets

$$\begin{pmatrix}
(e^{\pi\Gamma} - 1) - \pi\alpha(e^{\pi\Gamma} + 1) & -\pi\beta(1 - e^{\pi\Gamma}) \\
-\pi\beta(1 + e^{\pi\Gamma}) & (e^{\pi\Gamma} + 1) - \pi\alpha(e^{\pi\Gamma} - 1)
\end{pmatrix}
\begin{pmatrix}
\cos(\pi E) \\
\sin(\pi E)
\end{pmatrix} = 0.$$
(66)

This equation has a solution, when the determinant of the matrix vanishes. This condition gives

$$\Gamma = \frac{1}{2\pi} \ln \left(\frac{(\pi\alpha + 1)^2 + (\pi\beta)^2}{(\pi\alpha - 1)^2 + (\pi\beta)^2} \right) . \tag{67}$$

Eq. (67) has no singularity when $\beta \neq 0$. This means, the singularity in the widths of the resonances, obtained for $\beta = 0$ in Eqs. (27) vanishes when $\beta \neq 0$.

This result can be understood as follows. In [15] the distribution of exceptional points is investigated for systems described by a Hamiltonian of the type $\tilde{H} = H^0 + \tilde{\alpha}H^1$. The exceptional points of such a system are those points in the parameter space of $\tilde{\alpha}$ at which two (or more) eigenvalues coincide (for a more detailed discussion see for example [16]). The coupling constant $\tilde{\alpha}$ can be a real, imaginary or, more generally, a complex number. The distribution of the exceptional points is determined by the matrices H^0 and H^1 . It is independent of the value of $\tilde{\alpha}$ which determines, for its part, the positions of the (in general complex) eigenvalues of \tilde{H} . In the one-channel case (in which H^1 has rank one), there exist M-1 exceptional points corresponding to the crossing of the collective state with each of the other M-1 states.

For systems which show a phase transition, $all\ M-1$ exceptional points converge to the finite purely real value of $\tilde{\alpha} = \tilde{\alpha}_{\rm crit}$ in the limit $M \to \infty$. For finite systems, almost all exceptional points are near to this accumulation point. This result holds not only for the ideal picket fence, but for all systems, which suffer a phase transition [15].

For the systems investigated in the present paper it follows. The accumulation point being determined by the matrices H^0 and VV^T , is independent of the coupling parameter α . When the system with a purely imaginary coupling (i.e. $\beta=0$) shows a phase transition, all (M-1) exceptional points are met if α approaches the critical value. The collective mode repels with all the other ones simultaniously, i.e. all states run through their exceptional point at $\alpha=\alpha_{\rm crit}$. This means all M-1 exceptional points are accumulated at $\alpha_{\rm crit}$. In that case, $\langle \Phi_i | \Phi_i \rangle$ diverges for all i simultaneously in the limes $\alpha \to \alpha_{\rm crit}$. In fact, the dimension of the eigenspace collapses from N to 1 $(|\Phi_i\rangle=|\Phi_j\rangle$ $\forall i,j)$ if α hits the accumulation point. Therefore, also B diverges at $\alpha_{\rm crit}$. If the coupling parameter is complex $(\beta \neq 0)$, however, the system passes the accumulation point in a certain distance in the complex (α,β) -plane. As a result, the singularity at $\alpha_{\rm crit}$ will be avoided. For $|\alpha|\approx |\alpha_{\rm crit}|$, the quantity B does not diverge if $M\to\infty$ but reaches a certain maximum value. Refering to this result, we claim that, according to a rigorous mathematical definition, the phase transition will be destroyed by any given nonvanishing real part β in the coupling parameter (a detailed discussion of this aspect is given in [15]).

Let us illustrate this result by means of a numerical study. To that purpose, we replace α by $\alpha \cdot e^{i\varphi}$. We choose M=2N+1=101, as usually, and perform the calculations for $\varphi=1^0,10^0,45^0,80^0,89^0$ by varying α . The eigenvalues of \mathcal{H}^0 (for $\beta=0$) and the coupling matrix elements are chosen to be $E_k=k$ and $v_k=1$, respectively. In Fig. 8.a. we have drawn the number of principal components of the collective resonance state as a function of α .

The numerical results show a clear difference between the cases with small and large angle φ . The larger φ , the less is the number of basis states contributing to the collective state at a given $\alpha > \alpha_{\rm crit}$. Further, the curves rise up more smoothly when φ is larger. For large angles the maximum value $N_0^p=1$ is not reached at the maximum value $\alpha=2$ shown in the figure. Thus, in the case of the finite spectrum studied numerically, the reorganisation process is getting smoother the larger φ . In other words, the reorganisation process is washed out, if the system cannot hit the accumulation point of the exceptional points, but has to pass it in a certain distance in the complex parameter space.

This conclusion is underlined by the results given in Fig 8.b. Here we have fixed the angle φ to 45^0 and varied the number of states included in the spectrum (M=101 and 1001 states). As one can see, the characteristic features of the curves are not changed by changing the number

of basis states. The transition remains smooth also for N=1001 states over the whole range of α . So, these systems can not be characterized by a critical point. We see a critical region of α , which will be the larger, the larger the nearest distance between the accumulation point and the eigenvalues in the complex plane is.

5 Discussion of the results

The analytical and numerical investigations represented in the foregoing sections point to similarities and differences in the behaviour of the different systems under the influence of varying strength of the coupling to the continuum (decay channel). In any case, a restructuring in the system takes place (or starts to take place) when the coupling parameter α is large enough. A collective state which is aligned with the decay channel is formed in the centre of the spectrum. Its wavefunction is coherently mixed in the set of basis wavefunctions of the corresponding closed system. The trapped states have incoherently mixed wavefunctions. Beyond a certain value of the control parameter α , two different time scales exist (bifurcation of the widths).

In some cases, the restructuring in the system can be identified as a second-order phase transition. The separation of different time scales occurs suddenly at a critical value $\alpha_{\rm crit}$ and is a collective effect of the *whole* spectrum. The order parameter Γ_0/M increases linearly as a function of the control parameter α with a universal slope one, as soon as the control parameter is larger than its critical value. In other cases, the separation of time scales occurs successively by individual trapping of neighbouring resonance states. In that case, the collectivity is restricted by the extension of the energy region, overlapped by the fast decaying resonance state. The process of reorganisation continues up to $\alpha \to \infty$.

The differences in the behaviour of systems which show a phase transition to those which do not, can be seen nicely in the example of the ideal picket fence. In the case with equally distributed levels coupled with the same strength to one common channel, all states are equivalent. Consequently, the direction of the energy shift accompanying the local resonance trapping is undefined and the local resonance trapping is hindered. The redistribution of the system under the influence of the decay channel can take place only collectively. The quantity Γ_0/M rises linearly in $\alpha > \alpha_{\rm crit}$ with slope 1.

More realistic systems show a phase transition when the energy dependence of the level density is compensated by an energy dependence of the coupling strength. For example, a dilution of the level density can be compensated by a corresponding enhancement of the coupling strength. The critical value $\alpha_{\rm crit}$ is well determined. Further when the system is bounded from below, a phase transition occurs under the same conditions as for non-bounded systems. It occurs at the same critical value $(r+1)/\pi$.

Moreover we could show, that the conditions for a phase transition do not have to be fulfilled strictly, but only on the average. Small irregularities in the energy dependence of the levels or in the distribution of the coupling vectors are washed out, if the number of states in the spectrum is sufficiently high. Also the generic case of GOE-distributed states shows the features of a phase transition even for a comparably small number of states. The fast decaying state is created by all states of the spectrum, independently of whether they are overlapped by it or not.

Another characteristic feature of the phase transition is the mixing of the wavefunctions. In the case of the ideal picket fence, it changes suddenly at $\alpha_{\rm crit}$ from its minimum value $N_0^p=1/M$ to the maximum value $N_0^p=1$ for the state i=0. The width of the collective resonance state at $\alpha=\alpha_{\rm crit}$ is of the order of $\ln(M)$ whereas the extension of the spectrum is equal to M. Also in the more general case, where the energy dependence of the level density is compensated by the coupling strength of the resonance states, we could prove, that the width of the collective state is much smaller than the extension of the spectrum for couplings close to the critical point. Nevertheless, the collective state carries contributions of (almost) all basis states even if they are, in the case of a finite spectrum, close to the borders. When $\alpha \neq \alpha_{\rm crit}$, the value of N_0^p is independent of α . This holds also if the system is disturbed by random pertubations, where the compensation conditions are fulfilled only on the average.

The situation is different if the energy dependence of the level density is not compensated by the energy dependence of the coupling vector. In such a case, the local resonance trapping between neighbouring states is not hindered but occurs successively starting in the region with the largest level density or coupling strength. If the level density is larger in the centre of the spectrum than at other energies and the coupling strength to the channel is the same for all levels, the collective mode is created only locally for any finite value of α . This local collective state traps successively more and more resonance states in direction to the border of the spectrum. This process of local resonance trapping with increasing width of one state in the centre continues endlessly up to $\alpha \to \infty$ (in the limit $M \to \infty$). Although the short-lived state has collective properties it is not created by all basis states of the spectrum but only by those which are overlapped by it. There is no phase transition at all.

The resonance structure of the system is, in the cases considered, symmetrical in relation to the critical value $\alpha_{\rm crit}$ of the control parameter although the number of long-lived resonance states for $\alpha < \alpha_{\rm crit}$ and for $\alpha > \alpha_{\rm crit}$ differs by 1. As an example, the picket-fence distribution with level distance 1 and equal coupling strength to the continuum remains a picket-fence distribution also at $\alpha > \alpha_{\rm crit}$ but is shifted in energy by 1/2 of the level distance.

For finite M, collective states may be caused also by an additional real part to the Hamiltonian, e.g. $\mathcal{H}' = \mathcal{H}^0 + \beta V V^+$, leaving \mathcal{H}' hermitian. It is called internal collectivity in contrast to the external collectivity discussed above. In such a case, the process of reorganization in the system occurs smoothly. A phase transition does not take place. The eigenfunctions of \mathcal{H}' are orthogonal in the usual manner: $\langle \Phi'_i | \Phi'_i \rangle = 1$ for all i and α .

Also the non-hermiticity of the Hamiltonian \mathcal{H} is, however, not sufficient for the appearance of a phase transition, as the results presented in the foregoing sections show. In any case, the value B characterizing the bi-orthogonality of the set of eigenfunctions of \mathcal{H} plays a decisive role. Only when it becomes essentially, i.e. when $B \gg 1$ (see Eq. (23)) at a certain well-defined value of α , a phase transition takes place. When, however, the reordering of the system takes place successively in a limited region of the spectrum with $n \ll M$ states, then $B^{(n)} \equiv \frac{1}{n} \sum_{i=1}^{n} \langle \Phi_i | \Phi_i \rangle > 1$ but B is close to 1. In this case, the reorganisation in the system does not occur collectively but smoothly as a function of α .

As a result, in the case of a phase transition the bi-orthogonality of all the eigenfunctions of \mathcal{H} is maximal at (almost) the same value of α and, according to Eq. (23), $B \gg 1$ at $\alpha_{\rm crit}$. For illustration we show in Fig. 9 the value of B as a function of α for four different cases.

The theoretical value of $\alpha_{\rm crit}$ is marked by a vertical solid line. Only in the case without phase transition, this sum is always very close to 1 while it has a clearly expressed maximum at the critical point $\alpha_{\rm crit}$ whenever a phase transition occurs. Further, the eigenfunctions of \mathcal{H} are orthogonal in the usual manner for $\alpha \ll \alpha_{\rm crit}$ as well as for $\alpha \gg \alpha_{\rm crit}$. Here, $B \approx 1$.

This result can nicely be illustrated by means of the exceptional points defined as the crossing points of resonance states. They are determined by the structure of the different parts of the effective Hamiltonian (see sect. 4.4) but are independent of the coupling parameter. In the one-channel case considered by us, they accumulate at one point in the limit $M \to \infty$. In the case the system shows a phase transition, the eigenvalues meet this accumulation point when considered as a function of the coupling parameter and $B \to \infty$ in its neighbourhood.

Therefore, we may differentiate between four situations: (i) the exceptional points accumulate at a finite real value in the complex (α, β) -plane and the system goes through the accumulation point, (ii) the exceptional points accumulate at a finite real value in the complex (α, β) -plane but the phase φ of the coupling hinders the system to hit the accumulation point, (iii) the exceptional points accumulate at $\alpha, \beta = 0$, (iv) the exceptional points do not accumulate at all but they are spread over the whole complex (α, β) -plane with diverging absolute value of the coupling parameter. Examples are (i) the compensated case, (ii) the system with complex coupling, (iii) the overcompensated case, (iv) the undercompensated case (for details see [15]).

The stochastic processes described by the (complex) partial widths are much larger for $\alpha \approx \alpha_{\rm crit}$ than at other values of α . This is expressed by the relation $\Gamma_i = \gamma_{ic}/\langle \Phi_i | \Phi_i \rangle$ where γ_{ic} is the partial width of the state i in relation to the (only) decay channel c [1]. Since $\langle \Phi_i | \Phi_i \rangle \gg 1$ near $\alpha_{\rm crit}$, it follows $\Gamma_i \ll \gamma_{ic}$ for $\alpha \approx \alpha_{\rm crit}$. The structure observed in the cross section is determined by the S-matrix, Eq. (4). It depends essentially, according to Eq. (4), on the length of the spectrum (i.e on the values γ_{ic} of all the states), but not on the width $\Gamma_{i=0}$ of the collective state. For illustration, $\overline{|1-S_{11}|^2}$ is shown in Fig. 10 for three different values of $\alpha \geq \alpha_{\rm crit}$. The width of the collective state is $\Gamma_0/2=0.84$, 1.09 and 19.9, respectively, for the three values of α considered. The width Γ_0 has almost nothing in common with the structure observed in the cross section as one easily sees from the figure.

The same result follows also from our analytical considerations. At the critical point, the sum of the widths of all states is smaller than the total length M=2N+1 of the spectrum by a factor π according to Eq. (33). Furthermore, the width of the broadest state (in the centre of the spectrum) is in the order of $\ln N$ in the ideal picket-fence model. In the limit of large N it is in general tiny compared to the length of the spectrum according to Eq. (64). This shows, that the transition is caused by the cooperative behaviour of all states. It is *not* caused by the overlap of the complete spectrum by one of the states. In the cross section, we see a structure of the extension of the length of the spectrum since *all* states are coupled to the decay channel. The width of the broadest state is much smaller than this structure.

The numerical results show further that the number M of states need not necessarily be infinite in deciding the question whether the transition is of second order or not. The second-order phase transition is well expressed already for a relatively small number of states (M=2N+1=101 up to 1001 in our calculations) in all cases in which the analytical study shows a phase transition in the limit $M\to\infty$.

In our analytical and numerical studies the limiting case $M \to \infty$ is achieved by an extension of the length of the spectrum. It is worthwhile to note that the results are the same if, instead, the length of the spectrum is kept fixed at some finite value and the level density approaches ∞ with $M \to \infty$.

In many-particle systems, the level density depends on energy. In nuclei, it increases exponentially with energy. The coupling strength of the states to the continuum decreases, however, with energy due to the increasing contribution of many-particle many-hole configurations to the wavefunctions of the states ("compound nucleus states"). It is an interesting question whether in such a system the increasing level density is "compensated" in a certain energy range of the spectrum by the decreasing mean coupling strength so that the condition for a second-order phase transition is fulfilled.

Acknowledgment: We gratefully acknowledge valuable discussions with F. Leyvraz. C. Jung thanks CONACYT for a beca patrimonial. The work is supported by DAAD and DFG.

References

- P. Kleinwächter and I. Rotter, Phys. Rev. C 32, 1742 (1985); I. Rotter, Rep. Prog. Phys. 54, 635 (1991)
- [2] V.V. Sokolov and V.G. Zelevinsky, Phys. Lett. B 202, 10 (1988); V.V Sokolov and V.G. Zelevinsky, Nucl. Phys. A 504, 562 (1989)
- [3] F.M. Dittes, H.L. Harney and I. Rotter, Phys. Lett. A 153, 451 (1991)
- [4] W. Iskra, M. Müller and I. Rotter, J. Phys. G 19, 2045 (1993); G 20, 775 (1994)
- [5] M. Müller, F.-M. Dittes, W. Iskra and I. Rotter, Phys. Rev. E 52, 5961 (1995)
- [6] V.V. Sokolov, I. Rotter, D.V. Savin and M. Müller, Phys. Rev. C 56, 1031 and 1044 (1997)
- [7] H. Friedrich and D. Wintgen, Phys. Rev. A 32, 3231 (1985); A. Bürgers and D. Wintgen,
 J. Phys. B 27, L131 (1994)
- [8] N.E. Karapanagioti, O. Faucher, Y.L. Shao, D. Charalambidis, H. Bachau and E. Cormier, Phys. Rev. Lett. 74, 2431 (1995); N.Y. Kylstra and C.J. Joachain, Europhys. Lett. 36, 657 (1996)
- [9] F. Remacle, M. Munster, V.B. Pavlov-Verevkin and M. Desouter-Lecomte, Phys. Lett. A 145, 365 (1990); K. Someda, H. Nakamura and F.H. Mies, Chem. Phys. 187, 195 (1994);
 F. Remacle and R.D. Levine, J. Phys. Chem. 100, 7962 (1996); M. Desouter-Lecomte and J. Liévin, J. Chem. Phys. 107, 1428 (1997)
- [10] Y.V. Fyodorov and H.J. Sommers, J. Math. Phys. 38, 1918 (1997)
- [11] E. Persson, K. Pichugin, I. Rotter and P. Seba, to be published

- [12] H. Feshbach, Ann. Phys. (NY) 5 357 (1958); 19 287 (1962)
- [13] C. Mahaux and H.A. Weidenmüller, Shell model approach to nuclear reactions, North-Holland 1969
- [14] H. Haken, Advanced Synergetics, Springer-Verlag, 1983
- [15] W.D. Heiss, M. Müller, and I. Rotter, to be published
- [16] W.D. Heiss and A.L. Sannino, J. Phys. A 23, 1167 (1990)

Figure captions

Fig. 1.

Numerical illustration of Eq. (45) for different values of N and Γ in the positive energy range. (a) $\Gamma = 1, N = 500$ (full line), 1000 (dashed line), 5000 (dash-dotted line), (b) $N = 1000, \Gamma = 0.5$ (full line), 0.75 (dashed line), 1.0 (dash-dotted line). For details see text.

Fig. 2.

(a) The motion of the eigenvalues λ_k in the complex plane with increasing α for the ideal picket fence (N=50). The ordinate represents the values of $\Gamma_k/2$ while the abcisse those of \mathcal{E}_k . The full line shows the behaviour of Eq. (41). Only a part of the spectrum is shown. (b) $\Gamma_k/2$ as a function of α for N=50. (c) N_0^p as a function of α for N=50 (full line), 150 (dotted line).

Fig. 3

(a) Eigenvalues $\lambda_k = \mathcal{E}_k - i/2 \; \Gamma_k$ in the complex plane for a small energy range around the centre. $E_k = k \; \forall k \; \text{and} \; v_k = 1 \; \forall k \; \text{but} \; v_0 = 0.5. \; N = 50 \; \text{(rhombs)}, \; 150 \; \text{(crosses)}.$ (b) Γ_k as a function of (α) . $E_k = k \; \forall k \; \text{and} \; v_k = 1 \; \forall k \; \text{but} \; v_0 = 0.5. \; N = 50, 150.$

Fig. 4

Numerical illustration of Eq. (49). $\pi\mu \coth(\pi\mu) + D$ (left ordinate scale) for D = -0.5, 0, 0.5 (full lines) and μ/α (right ordinate scale) for different α . (a) for $\alpha = 0.1$ (dashed line), $1/\pi$ (solid thin line). (b) for $\alpha_{\rm crit} < \alpha < \alpha_{c2}$ (solid thin line), $\alpha \approx \alpha_{c2}$ (dashed line), $\alpha > \alpha_{c2}$ (dash-dotted line). For details see text.

Fig. 5

Number N_0^p of principal components as a function of α for the three different picket-fence distributions with $v_0 = 0.5, N = 50$ (dashed line), $v_0 = 1, N = 50$ (full line), and $v_0 = 2, N = 50$

(dash-dotted line), 150 (double-dotted-dashed line).

Fig. 6

 $\Gamma_k/2$ as a function of α for N=50. (a) $E_k=\operatorname{sign}(k)$ k^2 , $v_k=1$ $\forall k$, (b) $E_k=\operatorname{sign}(k)$ k^2 , $v_k^2=|k|+1$, (c) $E_k=\operatorname{sign}(k)$ k^2 , $v_k=|k|+1$, (d) E_k distributed according to an unfolded GOE, v_k are Gaussian distributed with mean value 1 and variance 0.1.

Fig. 7

 N_0^p as a function of α for (a) $E_k = \text{sign}(k) \ k^2$, $v_k = 1 \ \forall k, \ N = 50$ (full line), 150 (dashed line); (b) $E_k = \text{sign}(k) \ k^2$, $v_k^2 = |k| + 1$, N = 50 (full line), 150 (dotted line), 500 (dashed line); (c) $E_k = \text{sign}(k) \ k^2$, $v_k = |k| + 1$, N = 50 (full line); (d) E_k distributed according to an unfolded GOE, v_k are Gaussian distributed with mean value 1 and variance 0.1. N = 50 (full line), 150 (dotted line), 250 (dashed line), 500 (dash-dotted line).

Fig. 8

 N_0^p as a function of α for a system with complex coupling. Simultaneously, β changes according to $\beta = \alpha \tan(\varphi)$. (a) The values $\varphi = 1^0, 10^0, 45^0, 80^0, 89^0$ are shown as full, long-dashed, short-dashed, dotted, dash-dotted line, respectively. N = 50. (b) $\varphi = 45^0, N = 50$ (full line), N = 150 (dotted line).

Fig. 9

The value of B, Eq. (23), as a function of α . The thick full line shows the case $E_k = \text{sign}(k) \ k^2$, $v_k = 1 \ \forall k, N = 50$, thin solid line the ideal picket fence for N = 50, dashed line the ideal picket fence for N = 150, dash-dotted line the unfolded GOE as in Fig. 7.d for N = 150.

Fig. 10

 $\overline{|1-S_{11}|^2}$ for $\alpha=1/\pi$ (full line), $1/\pi+0.05$ (dashed line), $1/\pi+0.1$ (dash-dotted line). For comparison: $\Gamma_0/2=0.84$ for $\alpha=1/\pi$, $\Gamma_0/2=1.09$ for $\alpha=1/\pi+0.05$ and $\Gamma_0/2=19.9$ for $\alpha=1/\pi+0.1$.

This figure "fig1a.gif" is available in "gif" format from:

This figure "fig1b.gif" is available in "gif" format from: http://arXiv.org/ps/quant-ph/9804020v1

This figure "fig2a.gif" is available in "gif" format from:

This figure "fig2b.gif" is available in "gif" format from:

This figure "fig2c.gif" is available in "gif" format from:

This figure "fig3a.gif" is available in "gif" format from:

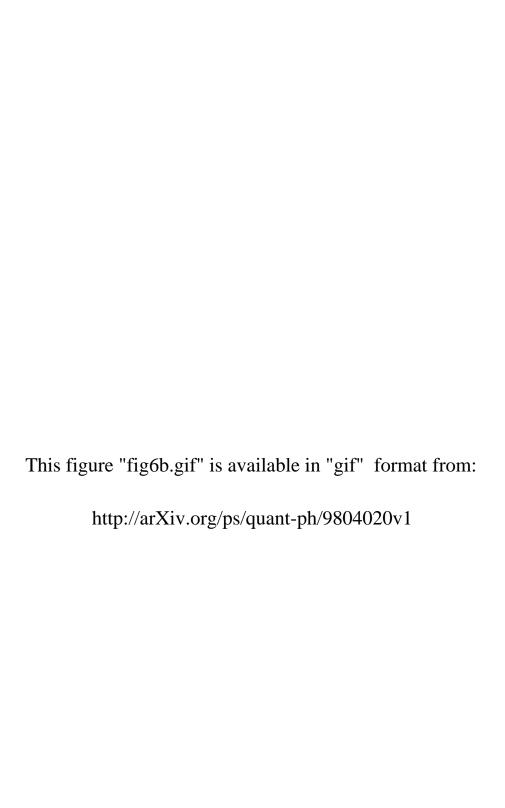
This figure "fig3b.gif" is available in "gif" format from:

This figure "fig4a.gif" is available in "gif" format from:

This figure "fig4b.gif" is available in "gif" format from:

This figure "fig5.gif" is available in "gif" format from:

This figure "fig6a.gif" is available in "gif" format from:



This figure "fig6c.gif" is available in "gif" format from:

This figure "fig6d.gif" is available in "gif" format from: http://arXiv.org/ps/quant-ph/9804020v1

This figure "fig7a.gif" is available in "gif" format from:

This figure "fig7b.gif" is available in "gif" format from:

This figure "fig7c.gif" is available in "gif" format from:

This figure "fig7d.gif" is available in "gif" format from:

This figure "fig8a.gif" is available in "gif" format from:

This figure "fig8b.gif" is available in "gif" format from: http://arXiv.org/ps/quant-ph/9804020v1

This figure "fig9.gif" is available in "gif" format from:

This figure "fig10.gif" is available in "gif" format from: